

## The Counterion Effect on the Assembly of Coordination Networks of Cationic ( $\eta^3$ -Allyl)palladium Complexes Containing 3,5-Dimethyl-4-nitro-1*H*-pyrazole

by Mercedes Cano\*<sup>a</sup>), José V. Heras<sup>a</sup>), M. Luz Gallego<sup>a</sup>), Josefina Perles<sup>b</sup>), Caridad Ruiz-Valero<sup>b</sup>), Elena Pinilla<sup>a</sup>), and M. Rosario Torres<sup>c</sup>)

<sup>a</sup>) Departamento de Química Inorgánica I, Facultad de Ciencias Químicas, Universidad Complutense, E-28040 Madrid (phone: +34 91 3944340; fax: +34 91 3944352; e-mail: mmcano@quim.ucm.es)

<sup>b</sup>) Departamento de Síntesis y Estructura de Óxidos, Instituto de Ciencia de Materiales de Madrid, CSIC, Cantoblanco, E-28049 Madrid

<sup>c</sup>) Laboratorio de Difracción de Rayos-X, Facultad de Ciencias Químicas, Universidad Complutense, E-28040 Madrid

Two new ( $\eta^3$ -allyl)palladium complexes containing the ligand 3,5-dimethyl-4-nitro-1*H*-pyrazole (Hdmpz) were synthesized and characterized as  $[\text{Pd}(\eta^3\text{-C}_3\text{H}_5)(\text{Hdmpz})_2]\text{BF}_4$  (**1**) and  $[\text{Pd}(\eta^3\text{-C}_3\text{H}_5)(\text{Hdmpz})_2]\text{NO}_3$  (**2**). The structures of these compounds were determined by single-crystal X-ray diffraction to evaluate the intermolecular assembly. Each complex exhibits similar coordination behavior consistent with cationic entities comprised of two pyrazole ligands coordinated with the  $[\text{Pd}(\eta^3\text{-C}_3\text{H}_5)]^+$  fragment in an almost square-planar coordination geometry. In **1**, the cationic entities are propagated through strong intermolecular H-bonds formed between the pyrazole NH groups and  $\text{BF}_4^-$  ions in one-dimensional polymer chains along the *a* axis. These chains are extended into two-dimensional sheet networks *via* bifurcated H-bonds. New intermolecular interactions established between  $\text{NO}_2$  and Me substituents at the pyrazole ligand of neighboring sheets give rise to a three-dimensional network. By contrast, compound **2** presents molecular cyclic dimers formed through  $\text{N-H}\cdots\text{O}$  H-bonds between two  $\text{NO}_3^-$  counterions and the pyrazole NH groups of two cationic entities. The dimers are also connected to each other through  $\text{C-H}\cdots\text{O}$  H-bonds between the remaining O-atom of each  $\text{NO}_3^-$  ion and the allyl  $\text{CH}_2$  H-atom. Those interactions expand in a layer which lies parallel to the face (101).

**Introduction.** – There is continuing interest in the crystal engineering of metal complexes. Because the supramolecular synthetic approach permits the design of arrays whose dimensions are greater than those of the molecular level found in the traditional covalent chemistry [1], this approach is now used for coordination polymers which have proved to show good electronic communication between metal centers. Coordinative and H-bonding interactions have been extensively exploited when looking for the assembly of coordination networks [2]. In this context, it has also been established that, when cationic and anionic complexes are used as building blocks, their corresponding counterions should play a crucial role in the determination of the architectures [2b][3]. Therefore, by considering metal-cationic complexes with functionalized H-bonding ligands, the contribution of selected counterions should be expected to support the assembly process.

In previous work in our laboratory, we have found a polymeric structure for  $[\text{Pd}(\eta^3\text{-C}_3\text{H}_5)(\text{HPz}^{\text{bp}2})_2]\text{BF}_4$  ( $\eta^3\text{-C}_3\text{H}_5 = \eta^3$ -allyl,  $\text{HPz}^{\text{bp}2} = 3,5$ -bis(4-butoxyphenyl)-1*H*-pyrazole) produced by H-bonds between the counterion  $\text{BF}_4^-$  and the pyrazole NH group of cationic units [4]. As an extension of those results, we are now interested in

investigating new polymeric assemblies by using substituted pyrazole ligands. Because of the inherent coordination and the potential H-bonding donor/acceptor groups, the 3,5-dimethyl-4-nitro-1*H*-pyrazole (Hdmnpz) [5][6] was selected as ligand to construct new frameworks based on the cationic complex  $[\text{Pd}(\eta^3\text{-C}_3\text{H}_5)(\text{Hdmnpz})_2]^+$ . Moreover, to examine the effect of the counterion upon the intermolecular interactions and controlling the molecular assembly, the crystal structures of  $[\text{Pd}(\eta^3\text{-C}_3\text{H}_5)(\text{Hdmnpz})_2]\text{BF}_4$  (**1**) and  $[\text{Pd}(\eta^3\text{-C}_3\text{H}_5)(\text{Hdmnpz})_2]\text{NO}_3$  (**2**) were resolved. The results indicate that the supramolecular architectures of the complexes  $[\text{Pd}(\eta^3\text{-C}_3\text{H}_5)(\text{Hdmnpz})_2]\text{A}$  (A =  $\text{BF}_4$ ,  $\text{NO}_3$ ) can be extremely modified by considering the nature and geometry of counterions.

**Results and Discussion.** – Reaction of Hdmnpz and the complex  $[\text{Pd}(\eta^3\text{-C}_3\text{H}_5)(\text{S})_2]\text{X}$  (S = acetone) [7], prepared *in situ* from  $[\text{Pd}(\eta^3\text{-C}_3\text{H}_5)(\mu\text{-Cl})_2]$  and AgX (X =  $\text{BF}_4$ ,  $\text{NO}_3$ ), gave air-stable complexes **1** and **2** as pale yellow solids. Elemental analysis and IR and  $^1\text{H-NMR}$  spectroscopic data agree with the proposed formulations (see *Exper. Part*).

The IR spectra of both compounds exhibit  $\tilde{\nu}(\text{NH})$  absorption bands at *ca.* 3200–3000  $\text{cm}^{-1}$  for the pyrazole ligand, which were practically identical to those of the free ligand. Because Hdmnpz has proved to have strong intermolecular H-bonds [6], the observed  $\tilde{\nu}(\text{NH})$  frequencies of the complexes suggest the presence of similar associated NH bonds. The existence of intermolecular H-bonds in **1** and **2** was also evidenced by their X-ray structures, which will be described below. The  $\tilde{\nu}(\text{NO})$  stretching bands arising from the substituent at C(4) of the pyrazole appear at *ca.* 1509 and 1360  $\text{cm}^{-1}$ , both for the free ligand and the complexes. The remaining bands of the pyrazole ligand are observed in their characteristic ranges [8]. Moreover, **1** and **2** exhibit the frequencies  $\tilde{\nu}(\text{BF})$  and  $\tilde{\nu}(\text{NO})$  of the corresponding counterions at 1064 and 1040  $\text{cm}^{-1}$  ( $\text{BF}_4^-$ ) and 1384 and 1361  $\text{cm}^{-1}$  ( $\text{NO}_3^-$ ). The splittings of these bands agree with the change in symmetry of these groups as a consequence of their interactions with the pyrazole ligand [4][9].

The  $^1\text{H-NMR}$  spectra ( $\text{CDCl}_3$ ) of **1** and **2** at room temperature are similar. The pattern of the pyrazole and allyl signals indicates a highly symmetric structure with only one type of pyrazole ligand. The following features are observed: *i*) there are two well-resolved *d* at  $\delta$  *ca.* 4.16 and 3.29, corresponding to the ‘*syn*’ and ‘*anti*’ protons of the allyl ligand, as well as a *m* at  $\delta$  *ca.* 5.85 arising from the ‘*meso*’ proton of this ligand. These results are in agreement with the presence of a symmetric allyl ligand; *ii*) the presence of only one Me resonance for the two pyrazole ligands at  $\delta$  *ca.* 2.65 is also consistent with the equivalence of the two pyrazole ligands. This fact suggests the presence of a possible metallotropic equilibrium as has been established for related compounds [10].

*X-Ray Structures of 1 and 2.* Crystals suitable for single-crystal X-ray analysis were obtained for **1** and **2** after recrystallization from  $\text{CH}_2\text{Cl}_2/\text{hexane}$ . Selected bond distances and angles with their estimated standard deviations are listed in *Table 1*<sup>1)</sup>. The crystal structures of **1** and **2** reveal that the complexes are comprised of  $\text{BF}_4^-$  and

<sup>1)</sup> Arbitrary numbering; for systematic names, see *Exper. Part*.

Table 1. Selected Bond Distances [Å] and Angles [°] for **1** and **2**<sup>1</sup>. E.s.d. in parentheses

	<b>1</b>	<b>2</b>		<b>1</b>	<b>2</b>
Pd(1)–N(1)	2.119(5)	2.127(3)	N(1)–Pd(1)–N(3)	92.5(2)	94.0(1)
Pd(1)–N(3)	2.123(5)	2.108(4)	N(1)–Pd(1)–C(1)	99.1(3)	99.1(2)
Pd(1)–C(1)	2.110(8)	2.114(5)	N(1)–Pd(1)–C(2)	132.5(5)	130.5(2)
Pd(1)–C(2)	2.08(1)	2.087(6)	N(1)–Pd(1)–C(3)	168.7(3)	167.2(2)
Pd(1)–C(3)	2.138(8)	2.098(6)	N(3)–Pd(1)–C(1)	167.8(3)	166.0(2)
C(1)–C(2)	1.24(2)	1.309(8)	N(3)–Pd(1)–C(2)	134.8(5)	133.2(2)
C(2)–C(3)	1.31(2)	1.333(8)	N(3)–Pd(1)–C(3)	98.7(3)	98.8(2)
B(1)–F(1)	1.30(1)	–	C(1)–Pd(1)–C(2)	34.3(5)	36.3(2)
B(1)–F(2)	1.51(1)	–	C(1)–Pd(1)–C(3)	69.9(3)	68.2(2)
B(1)–F(3)	1.12(1)	–	C(2)–Pd(1)–C(3)	36.2(5)	37.1(2)
B(1)–F(4)	1.32(1)	–			
N(7)–O(5)	–	1.219(5)			
N(7)–O(6)	–	1.249(4)			
N(7)–O(7)	–	1.249(5)			

$\text{NO}_3^-$  ions and the cationic entity  $[\text{Pd}(\eta^3\text{-C}_3\text{H}_5)(\text{Hdmpz})_2]^+$ , bonded through strong H-bonds.

The structure of the mononuclear cations of **1** and **2** are similar, as shown in *Fig. 1, a and b*. In both cases, one crystallographic independent metal center interacts with two pyrazole ligands and an allyl ligand. The coordination geometry of the  $\text{Pd}^{\text{II}}$  ion is almost square-planar, similar to that observed in the previously described  $[\text{Pd}(\eta^3\text{-C}_3\text{H}_5)(\text{HPz}^{\text{bp}2})_2]\text{BF}_4$  complex [4]. Two pyrazole ligands coordinate to the  $\text{Pd}^{\text{II}}$  center *via* the corresponding unsaturated, atoms N(1) and N(3)<sup>1</sup>, with bond distances in the range of 2.11–2.13 Å. The allyl ligand exhibits Pd–C distances that range between 2.08 and 2.14 Å, in agreement with those observed in complexes containing N,N'-ligands *trans* to the allyl-palladium fragment [7][11]. Within each molecule, the nitro group is almost coplanar with the pyrazole ring (torsion angles O(1)–N(5)–C(11)–C(12) = 13(1)° and O(3)–N(6)–C(6)–C(7) = –4(1)° for **1** and O(2)–N(5)–C(11)–C(10) = 9.6(7)° and O(3)–N(6)–C(6)–C(7) = –0.6(7)° for **2**). By defining the coordination plane as that containing the Pd-atom and the two coordinating pyrazole N-atoms, the maximum deviation for the terminal allyl atom is 0.15(1) Å for **1** and 0.177(6) Å for **2**. The central allyl atom C(2) also deviates by 0.12(3) and 0.433(9) Å in **1** and **2**, respectively. However, the most-significant differences between these molecular cations are: *i*) the dihedral angle between the pyrazole planes, which is 40.6(2)° for **1** and 73.7(1)° for **2**, and *ii*) the dihedral angle formed by the plane of the allyl atoms C(1)–C(2)–C(3) and the plane Pd(1)–N(1)–N(3)–C(1)–C(3), 28(3)° and 61.0(7)°, respectively. Those features could be related to the different interactions of the pyrazole NH groups with the corresponding counterion  $\text{BF}_4^-$  in **1** and  $\text{NO}_3^-$  in **2**. In this context and for comparative purposes, we took into account the structural data of some allyl palladium derivatives containing pyrazolyl groups. These exhibited dihedral angles between the allyl ligand and the coordination plane Pd–N–N of 90° [11], 111.3° [7], or 113° and 108° [12], but all of them presented restricted positions on the pyrazole rings because of the characteristics of the polydentate ligands in which the pyrazolyl group was included, *i.e.*, in 4,6-bis(1*H*-pyrazol-1-yl)pyrimidine [11] and 4,6-bis(4-methyl-1*H*-pyrazol-1-

yl)1,3,5-triazin-2-olate [7], or by the coordinative form as bridging group in bis( $\eta^3$ -allyl)bis[ $\mu$ -(3,5-dimethyl-1*H*-pyrazolato-) $\kappa$ N<sup>1</sup>: $\kappa$ N<sup>2</sup>]]palladium(II) [12]. In our complexes, the position of the pyrazole ligands was constrained only by the H-bonding interactions with the corresponding counterion BF<sub>4</sub><sup>-</sup> in **1** and NO<sub>3</sub><sup>-</sup> in **2**, this fact, therefore, being related with the lower dihedral angles between the allyl and coordination planes (28(3)° and 61.0(7)° for **1** and **2**, resp.).

The molecular packing in **1** (Fig. 2, *a*) could be described as formed by polymer chains along the *a* axis, which interact with each other through N–H⋯F [13] and C–H⋯O [14] intermolecular H-bonds, giving rise to a three-dimensional network. In these chains, the cationic entities are propagated through two strong intermolecular H-bonds between the pyrazole NH groups and two neighboring BF<sub>4</sub><sup>-</sup> ions, N(2)–H⋯F(2) (with Footnote *b* in Table 2) and N(4)–H⋯F(1) (Table 2)<sup>1</sup>). Along the chains, the molecules are oriented in a head-to-head fashion, but they are in a head-to-tail relation with respect to the adjacent chains. The same BF<sub>4</sub><sup>-</sup> ion acts as a linkage between two cationic units from adjacent chains through bifurcated H-bonds, N(4)–H⋯F(2) (with Footnote *c* in Table 2), to construct a two-dimensional sheet network which propagates along the plane *ac*.

Table 2. Observed Hydrogen Bonding Interactions<sup>a</sup>) for **1** and **2**<sup>1</sup>). E.s.d. in parentheses.

	D–H⋯A	D⋯A	D–H	H⋯A	D–H⋯A
<b>1</b>	N(2)–H⋯F(2) <sup>b</sup> )	2.843(7)	0.86	1.98	176.1
	N(4)–H⋯F(1)	2.90(1)	0.86	2.22	135.4
	N(4)–H⋯F(2) <sup>c</sup> )	3.096(8)	0.86	2.51	125.9
	C(9)–H(B)⋯O(1) <sup>d</sup> )	3.44(1)	0.96	2.56	152.2
	C(9)–H(C)⋯O(4) <sup>e</sup> )	3.180(9)	0.96	2.60	118.9
	C(8)–H(C)⋯O(3) <sup>f</sup> )	3.34(1)	0.96	2.62	131.7
<b>2</b>	N(2)–H⋯O(6)	2.850(5)	0.90(5)	1.96(5)	168(4)
	N(4)–H⋯O(7) <sup>f</sup> )	2.764(5)	0.82(5)	1.95(5)	175(5)
	C(3)–H(B)⋯O(5)	3.167(8)	0.97	2.55	121.2

<sup>a</sup>) The values agree with those found for strong and weak related intermolecular H-bonding interactions [13][14]. <sup>b</sup>)  $x-1, y, z$ . <sup>c</sup>)  $x, -y+1/2, z+1/2$ . <sup>d</sup>)  $-x, -y, -z$ . <sup>e</sup>)  $-x+1, -y, -z+1$ . <sup>f</sup>)  $-x, -y, -z+1$ .

Because of the molecular arrangement, the NO<sub>2</sub> groups belonging to neighboring sheets lie in front of each other. That disposition is responsible for new intermolecular interactions C–H⋯O (Table 2) produced between the O-atoms of NO<sub>2</sub> substituents of the pyrazole ligand on one side of the sheet and the Me substituents of the pyrazole moiety from molecules located on contiguous sheets, giving rise to a three-dimensional network (Fig. 2, *a*).

From the viewpoint of topology, the structure of **1** could be visualized as containing planes of N-atoms and C-atoms from the pyrazole ligands as well as planes of NO<sub>2</sub> substituents with interlayer [Pd( $\eta^3$ -C<sub>3</sub>H<sub>5</sub>)]<sup>+</sup> fragments. The holes of that structure are occupied by BF<sub>4</sub><sup>-</sup> ions (Fig. 2, *b*).

The molecular packing of **2** shows significant differences. Thus, unlike the polymeric chains of **1**, compound **2** presents dimers produced through H-bonds between two cationic entities and two NO<sub>3</sub><sup>-</sup> ions. It could be visualized on the basis of the planar geometry of the NO<sub>3</sub><sup>-</sup> ions. Thus, two O-atoms of NO<sub>3</sub><sup>-</sup> interact through two

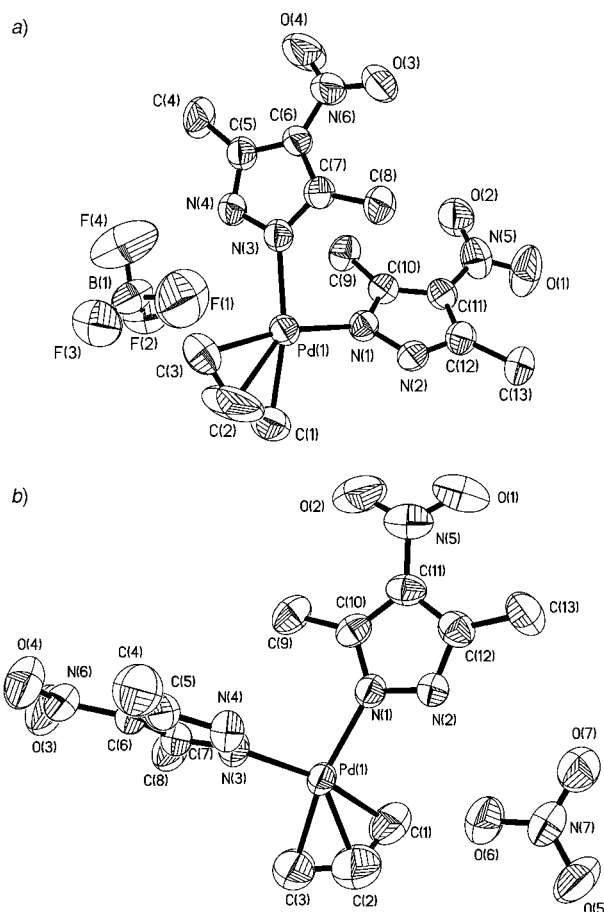


Fig. 1. Perspective ORTEP of a) **1** and b) **2** with the atomic numbering scheme<sup>1</sup>). H-Atoms are omitted for clarity, and thermal ellipsoids are at 50% probability level.

strong NH bonds (Table 2) with the pyrazole ligands of two different molecules, allowing the dimerization in a cyclic fashion (Fig. 3). This fact is reflected by the two equivalent N–O bond distances being longer than the third one (Table 1), the former ones corresponding to strong N–O⋯H interaction in the dimer. The third N–O bond distance of 1.219(5) Å is related to the remaining O-atom atom of the NO<sub>3</sub><sup>−</sup> ion, which is linked to a allyl CH<sub>2</sub> H-atom by an H-bond interaction C(3)–H(B)⋯O(5) (Table 2). These interactions expand in a layer, which lies parallel to the face (101) (Fig. 4).

**Conclusions.** – Cationic ( $\eta^3$ -allyl)palladium compounds containing *N*-unsubstituted pyrazole ligands and [BX<sub>*n*</sub>]<sup>−</sup> groups as counterions are designed to produce networks with strong N–H⋯X H-bonds. Although the nature and geometry of the counterion should control the molecular assembly, the substituents at the pyrazole ligands also

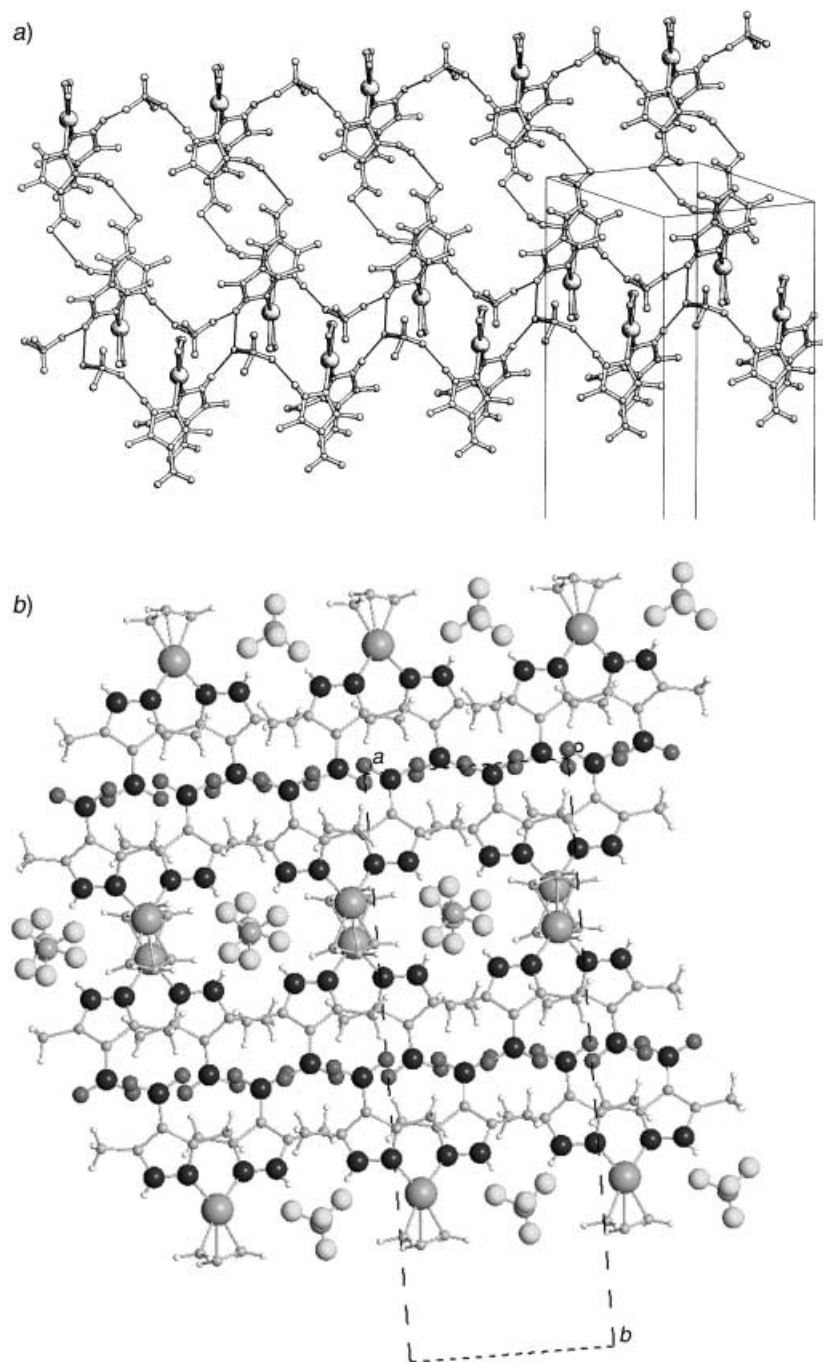


Fig. 2. a) Packing arrangement of **1** viewed along the *a* axis showing intermolecular  $N-H\cdots F$  and  $C-H\cdots O$  interactions; b) packing arrangement of **1** viewed through the *c* axis

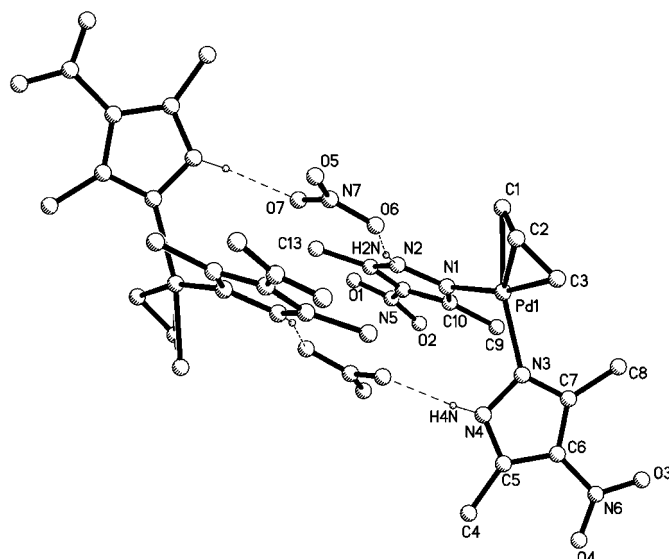


Fig. 3. PLUTO Plot of **2** with the atomic numbering scheme: dimer unit formed by intermolecular strong  $N-H \cdots O$  bonds<sup>1</sup>)

should be considered for these purposes. In this context, 3,5-dimethyl-4-nitro-1*H*-pyrazole was used to favor new potential interactions through the  $\text{NO}_2$  groups.

Compounds **1** and **2** are examples presenting strong H-bonds in the molecular assembly of cationic entities. Taking into account the nature and structural characteristics of the corresponding counterions,  $\text{BF}_4^-$  and  $\text{NO}_3^-$ , polymer chains or dimers, both extended to two-dimensional-sheet networks by new intermolecular H-bond interactions, are produced for **1** and **2**, respectively. However, the two-dimensional-sheet networks are clearly different. Thus, only in **1** are the sheets linked to each other by  $\text{C-H} \cdots \text{O}$  interactions between the  $\text{NO}_2$  and Me substituents of the pyrazole ligands, this network being made possible by the molecular orientation in the sheets.

Compounds **1** and **2** are examples of two- and three-dimensional H-bonding networks controlled by the characteristics of the counterion.

#### Experimental Part

*General.* The commercial starting material  $[\text{Pd}(\eta^3\text{-C}_3\text{H}_5)(\mu\text{-Cl})_2]$  was used as supplied. Ligand 3,5-dimethyl-4-nitro-1*H*-pyrazole (Hdmnpz) was prepared as described [15]. Commercial solvents were dried prior to use. IR Spectra: Nicolet Magna-550 FT-IR spectrophotometer; KBr pellets, 4000 – 400  $\text{cm}^{-1}$  region;  $\tilde{\nu}$  in  $\text{cm}^{-1}$ .  $^1\text{H-NMR}$  Spectra: Bruker AC-200 (200.13 MHz) spectrometer; performed by the Nuclear Magnetic Resonance Service of the Complutense University; chemical shifts  $\delta$  in ppm ( $\pm 0.1$  ppm) from  $\text{CDCl}_3$ , coupling constants  $J$  in Hz ( $\pm 0.3$  Hz). Elemental analyses for C, H, and N were carried out by the Microanalytical Service of the Complutense University.

*Bis(3,5-dimethyl-4-nitro-1*H*-pyrazole- $\kappa\text{N}^2$ )( $\eta^3$ -prop-2-enyl)palladium(1+) Tetrafluoroborate and Nitrate (**1** ( $\text{X}=\text{BF}_4$ ) and **2** ( $\text{X}=\text{NO}_3$ ), resp.).* AgX (0.18 mmol) was added under  $\text{N}_2$  to a soln. of  $[\text{Pd}(\eta^3\text{-C}_3\text{H}_5)(\mu\text{-Cl})_2]$  (33 mg, 0.09 mmol) in freshly distilled acetone (15 ml). After stirring for 6 h in the darkness, the soln. was

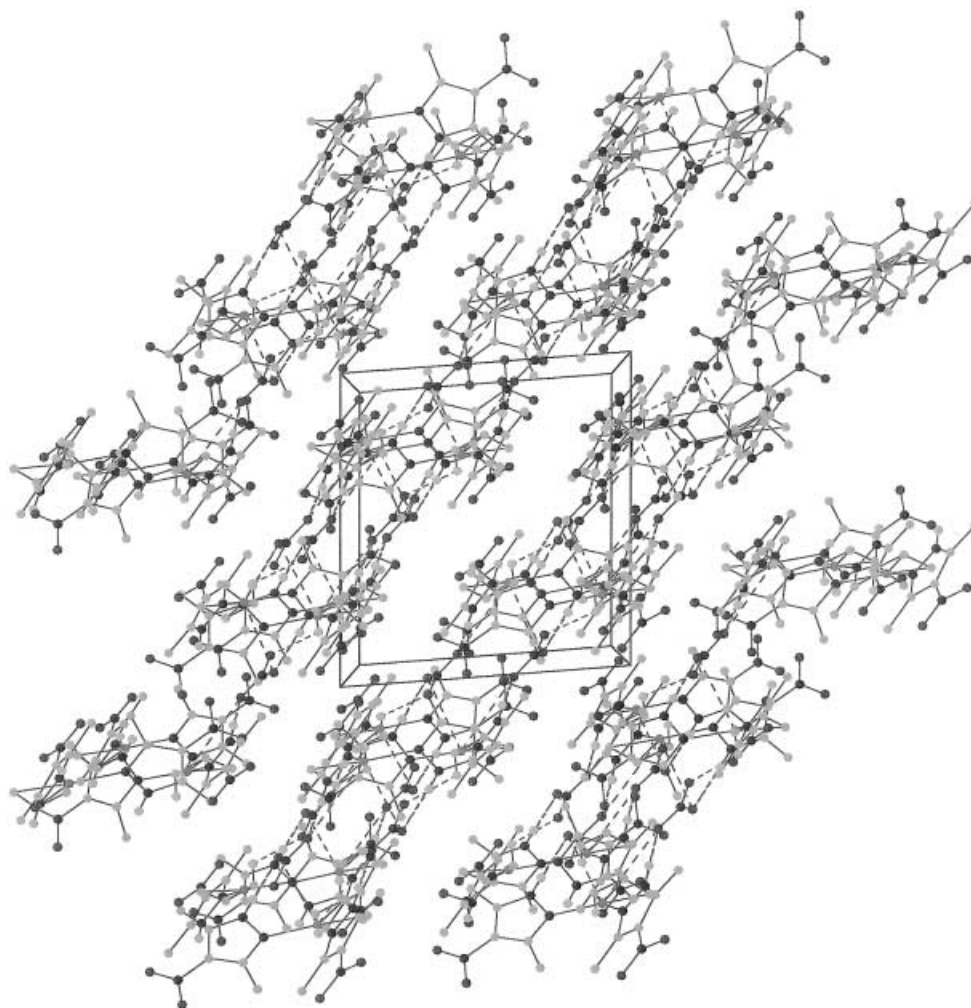


Fig. 4. Packing arrangement of **2** showing layers parallel to the face (101)

filtered through a plug of *Celite* and cooled with an ice bath. Then Hdmnpz (51 mg, 0.36 mmol) was added, and the mixture was stirred for 5 h. After evaporation, the white product crystallized from  $\text{CH}_2\text{Cl}_2$ /hexane.

*Data of 1:* Yield 31 mg (33%). IR (KBr): 3202–3069 (N–H), 1602 (C=N), 1503 (NO, as.), 1364 (NO, s.), 1064 and 1040 (BF).  $^1\text{H-NMR}$  (200.13 MHz,  $\text{CDCl}_3$ , 298 K): 5.88 (*m*,  $^3J_{\text{syn}} = 6.8$ ,  $^3J_{\text{anti}} = 12.7$ ,  $\text{H}_{\text{meso}}$ ); 4.19 (*d*,  $^3J_{\text{syn}} = 6.8$ , 2  $\text{H}_{\text{syn}}$ ); 3.34 (*d*,  $^3J_{\text{anti}} = 12.7$ , 2  $\text{H}_{\text{anti}}$ ); 2.60 (*s*, 4 Me). Anal. calc. for  $\text{C}_{13}\text{H}_{19}\text{BF}_4\text{N}_6\text{O}_4\text{Pd}$  (516.21): C 30.22, H 3.68, N 16.27; found: C 30.21, H 3.60, N 16.22.

*Data of 2:* Yield 33 mg (37%). IR (KBr): 3202–3065 (N–H), 1598 (C=N), 1515 (NO, as.), 1383 and 1361 (NO,  $\text{NO}_3$ ), 1361 (NO, s.).  $^1\text{H-NMR}$  (200.13 MHz,  $\text{CDCl}_3$ , 298 K): 5.83 (*m*,  $^3J_{\text{syn}} = 7.1$ ,  $^3J_{\text{anti}} = 12.4$ ,  $\text{H}_{\text{meso}}$ ); 4.13 (*d*,  $^3J_{\text{syn}} = 7.1$ , 2  $\text{H}_{\text{syn}}$ ); 3.24 (*d*,  $^3J_{\text{anti}} = 12.4$ , 2  $\text{H}_{\text{anti}}$ ); 2.66 (*s*, 4 Me). Anal. calc. for  $\text{C}_{13}\text{H}_{19}\text{N}_7\text{O}_7\text{Pd}$  (491.40): C 31.75, H 3.87, N 19.94; found: C 31.91, H 3.73, N 19.82.

*X-Ray Structure Determination.* Suitable crystals of compounds **1** and **2** for X-ray experiments were obtained from  $\text{CH}_2\text{Cl}_2$ /hexane. For both compounds, the data collection was carried out at r.t. on a *Bruker Smart-CCD* diffractometer with graphite-monochromated  $\text{MoK}\alpha$  radiation ( $\lambda$  0.71073 Å) operating at 50 kV



Table 3. *Crystal and Refinement Data for 1 and 2*

	<b>1</b>	<b>2</b>
Formula	[C <sub>13</sub> H <sub>19</sub> N <sub>6</sub> O <sub>4</sub> Pd]BF <sub>4</sub> <sup>-</sup>	[C <sub>13</sub> H <sub>19</sub> N <sub>6</sub> O <sub>4</sub> Pd]NO <sub>3</sub>
<i>M<sub>r</sub></i>	516.55	491.75
Temperature/K	296(2)	296(2)
Crystal system	monoclinic	monoclinic
Space group	<i>P</i> 2 <sub>1</sub> / <i>c</i>	<i>P</i> 2 <sub>1</sub> / <i>n</i>
<i>a</i> /Å	8.833(3)	10.8192(9)
<i>b</i> /Å	23.877(8)	15.193(1)
<i>c</i> /Å	10.089(3)	11.948(1)
$\beta$ /°	110.384(5)	94.362(2)
<i>V</i> /Å <sup>3</sup>	1994.5(11)	1958.4(3)
<i>Z</i>	4	4
<i>F</i> (000)	1032	992
Crystal size/mm	0.50 × 0.40 × 0.20	0.13 × 0.13 × 0.15
<i>d</i> <sub>calc</sub> /g cm <sup>-3</sup>	1.720	1.668
$\mu$ /mm <sup>-1</sup>	0.999	0.998
Scan technique	$\phi$ , $\omega$	$\phi$ , $\omega$
Data collected	(-13, -33, -10) to (13, 34, 14)	(-13, -13, -15) to (14, 20, 14)
$\theta$ /°	4.71 to 32.00	2.17 to 28.81
Reflections collected	14182	12296
Reflections independent	6013 ( <i>R</i> <sub>int</sub> = 0.1135)	4593 ( <i>R</i> <sub>int</sub> = 0.0456)
Data, restraints, parameters	6013, 0, 267	4593, 0, 199
G.o.f. ( <i>F</i> <sup>2</sup> )	0.741	0.902
Reflections obs. ( <i>P</i> > 2 $\sigma$ ( <i>I</i> ))	6013	4646
<i>R</i> <sub>1</sub> (reflections obs.) <sup>a</sup>	0.068	0.041
<i>R</i> <sub>w</sub> <sup>b</sup>	0.158	0.091

<sup>a</sup>  $R_1 = \sum [|F_o| - |F_c|] / \sum |F_o|$ . <sup>b</sup>  $Rw_F = \{ \sum [w(F_o^2 - F_c^2)^2] / \sum [w(F_o^2)^2] \}^{1/2}$ .

and 25 Å. Data were collected over a hemisphere of the reciprocal space by combination of three exposure sets. Each exposure of 20 s covered 0.3° in  $\omega$ . The cell parameters were determined and refined by least-squares fit of all reflections collected. The first 50 frames were recollected at the end of the data collection to monitor crystal decay, and no appreciable decay was observed. A summary of the fundamental crystal data and refinement parameters is given in *Table 3*.

The structures were solved by direct methods and refined by full-matrix least-squares on *F*<sup>2</sup> [16]. Anisotropic parameters were used in the last cycles of refinement for all non-H-atoms; for compound **2**, all O-atoms and the C-atoms of the allyl group were refined in only three anisotropic cycles, and, in subsequent cycles, their thermal parameters were kept constant. In both compounds, all H-atoms were included in calculated positions (rigid model), except H2N and H4N of compound **2**, bonded to N-atoms, which were located in a *Fourier* synthesis, included and refined its coordinates. Maximum and minimum peaks in a final difference synthesis were 1.44 and 0.65 eÅ<sup>-3</sup> for **1**, and 0.974 and 0.359 eÅ<sup>-3</sup> for **2**. In compound **1**, because of the non-resolvable disorder due to the thermal motion involving the BF<sub>4</sub><sup>-</sup> group, the *R* values and the maximum shift/error are higher than usual. This fact is common to compounds containing free BF<sub>4</sub><sup>-</sup> anions. CCDC-207445 (**1**) and -207446 (**2**) contain the supplementary crystallographic data for this paper. These data can be obtained free of charge via <http://www.ccdc.cam.ac.uk/conts/retrieving.html> (or from the *Cambridge Crystallographic Data Centre*, 12 Union Road, Cambridge CB2 1EZ, UK; fax: +44 1223 336033; e-mail: deposit@ccdc.cam.ac.uk).

We are indebted to *DGI/MCyT* of Spain for financial support (PB98-0766).

## REFERENCES

- [1] J. M. Lehn, 'Supramolecular Chemistry: Concepts and Perspectives', VHC, Weinheim, 1995; D. Philp, J. F. Stoddart, *Angew. Chem., Int. Ed.* **1996**, 35, 1155; J. Hamblin, L. J. Childs, N. W. Alcock, M. J. Hannon, *J. Chem. Soc., Dalton Trans.* **2002**, 164.
- [2] a) R. J. Smithson, C. A. Kilner, A. R. Brough, M. A. Halcrow, *Polyhedron* **2003**, 22, 725; S.-L. Zheng, M.-L. Tong, X.-M. Chen, S. W. Ng, *J. Chem. Soc., Dalton Trans.* **2002**, 360; N. S. Oxtoby, A. J. Blake, N. R. Champness, C. Wilson, *Proc. Natl. Acad. Sci. U.S.A.* **2002**, 99, 4905; M. Bakir, *Inorg. Chim. Acta* **2002**, 332, 1; b) J. Hamblin, A. Jackson, N. W. Alcock, M. J. Hannon, *J. Chem. Soc., Dalton Trans.* **2002**, 1635; M. A. Withersby, A. J. Blake, N. R. Champness, P. Hubberstey, W.-S. Li, M. Schröder, *Angew. Chem., Int. Ed.* **1997**, 36, 2327; M. A. Withersby, A. J. Blake, N. R. Champness, P. A. Cooke, P. Hubberstey, W.-S. Li, M. Schröder, *Crystal Engineering* **1999**, 2, 123; J. Yoo, Y.-K. Han, Y. S. Lee, Y. Do, *Polyhedron* **2002**, 21, 715; M. Bertelli, L. Carlucci, G. Ciani, D. M. Proserpio, A. Sironi, *J. Mater. Chem.* **1997**, 7, 1271; F. Adhami, M. Ghassemzadeh, M. M. Heravi, A. Taeb, B. Neumüller, *Z. Anorg. Allg. Chem.* **1999**, 625, 1411; C.-H. Chen, J. Cai, X.-L. Feng, X.-M. Chen, *Polyhedron* **2002**, 21, 689; I. Boldog, E. B. Rusanov, A. N. Chernega, J. Sieler, K. V. Domasevitch, *Polyhedron* **2001**, 20, 887.
- [3] M. Munakata, M. Wen, Y. Suenaga, T. Kuroda-Sowa, M. Maekawa, M. Anahata, *Polyhedron* **2001**, 20, 2037; M. Munakata, M. Wen, Y. Suenaga, T. Kuroda-Sowa, M. Maekawa, M. Anahata, *Polyhedron* **2001**, 20, 2321.
- [4] R. M. Claramunt, P. Cornago, M. Cano, J. V. Heras, M. L. Gallego, E. Pinilla, M. R. Torres, *Eur. J. Inorg. Chem.* **2003**, 2693.
- [5] G. A. Ardizzioia, S. Cenini, G. La Monica, N. Masciocchi, A. Maspero, M. Moret, *Inorg. Chem.* **1998**, 37, 4284.
- [6] C. Foces-Foces, F. H. Cano, J. Elguero, *Gazz. Chim. Ital.* **1993**, 123, 477.
- [7] F. Gómez-de la Torre, A. de la Hoz, F. A. Jalón, B. R. Manzano, A. Otero, A. M. Rodríguez, M. C. Rodríguez-Pérez, *Inorg. Chem.* **1998**, 37, 6606.
- [8] M. C. Torralba, M. Cano, J. A. Campo, J. V. Heras, E. Pinilla, M. R. Torres, *J. Organomet. Chem.* **2002**, 654, 150.
- [9] K. Nakamoto, 'Infrared and Raman Spectra of Inorganic and Coordination Compounds', 4th edn., Wiley, New York, 1986.
- [10] M. Cano, J. V. Heras, M. Maeso, M. Alvaro, R. Fernández, E. Pinilla, J. A. Campo, A. Monge, *J. Organomet. Chem.* **1997**, 534, 159; M. Cano, J. A. Campo, J. V. Heras, J. Lafuente, C. Rivas, E. Pinilla, *Polyhedron* **1995**, 14, 1139.
- [11] F. Gómez-de la Torre, A. de la Hoz, F. A. Jalón, B. R. Manzano, A. M. Rodríguez, *Inorg. Chem.* **2000**, 39, 1152.
- [12] G. W. Henslee, J. D. Oliver, *J. Cryst. Mol. Struct.* **1977**, 7, 137.
- [13] E. Goreschnik, M. Leblanc, E. Gaudin, F. Taulelle, V. Maisonneuve, *Solid State Sci.* **2002**, 4, 1213.
- [14] T. Steiner, *J. Chem. Soc., Perkin Trans. 2* **1995**, 1315.
- [15] G. T. Morgan, I. Ackerman, *J. Chem. Soc.* **1923**, 1308.
- [16] G. M. Sheldrick, 'SHELXTL97, Program for the Refinement of Crystal Structures', University of Göttingen, Germany, 1997.

Received April 16, 2003